

Thermoreversible Radial Growth of Micellar Assembly for Hydrogel Formation Using Zwitterionic Oligopeptide Copolymer

Bo Gyu Choi,^{†,‡} So-Hye Cho,[§] Hyesun Lee,^{†,‡} Myung Hwa Cha,[†] Kwideok Park,[†] Byeongmoon Jeong,^{*,‡} and Dong Keun Han^{*,†}

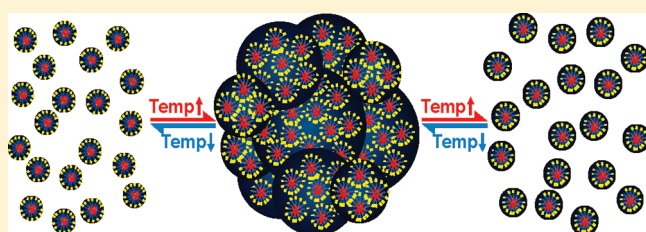
[†]Biomaterials Center, Korea Institute of Science and Technology, P.O. Box 131, Cheongryang, Seoul 130-650, Korea

[‡]Department of Chemistry and Nano Science and Department of Bioinspired Science (WCU), Ewha Womans University, 11-1 Seoul 120-750, Korea

[§]Nano-materials Center, Korea Institute of Science and Technology, P.O. Box 131, Cheongryang, Seoul 130-650, Korea

S Supporting Information

ABSTRACT: Amphiphilic block copolymers can self-assemble into micelles in water and can further form thermosensitive gels. Here, we explored Pluronic F127 ABA triblock copolymer of poly(ethylene glycol) (PEG; A) and poly(propylene glycol) (PPG; B), modified with telechelic ionic peptides, either anionic Gly-Phe-Gly-Asp (GFGD) or zwitterionic Gly-Arg-Gly-Leu (GRGL) or Gly-Arg-Gly-Asp (GRGD). All block copolymers formed micelles, but only those bearing zwitterionic peptides formed thermoreversible nanoassembly of micellar aggregates. These aggregates facilitate to form a gel at high polymer concentrations, thus making the sol-to-gel transition temperature lower than F127 and FGM. An increase in the sol-to-gel transition temperature and a decrease in the gel modulus have been a concern for biomedical applications of hydrophobically modified Pluronic. Current zwitterionic modified Pluronic F127, on the contrary, decreased the sol-to-gel transition temperature without loss of the gel modulus. The gelation, evidenced by cryo-transmission electron microscopy images, involves radial growth of micelle aggregates, which is strikingly different from that of Pluronic driven by simple unimer-to-micelle transition. The RGD-containing copolymer is of particular interest, in that it is cytocompatible and capable of binding to cell-surface adhesion receptors. This work suggests a new platform in designing a temperature-sensitive polymer with a unique nanoassembly for tissue regeneration.



INTRODUCTION

Self-assembly of amphiphilic block copolymers has been a basic tool in constructing nanostructures of organic and inorganic materials: e.g., mesoporous silica,¹ nano-ordered ceramics,² metal nanoparticles,³ supramolecular capsules,⁴ and polymeric nanocarriers for drugs.⁵ In particular, when a block copolymer has a balanced structure of hydrophilicity and hydrophobicity, the polymer aqueous solution exhibits a temperature-responsive assembly behavior.^{6,7} Pluronic F127 ABA triblock copolymer of poly(ethylene glycol) (PEG; A) and poly(propylene glycol) (PPG; B) is a well-known thermosensitive polymer. The aqueous solution of this polymer undergoes sol-to-gel transition as the temperature increases at a concentration higher than 16.0 wt %.⁸ The mechanism of the transition was suggested as a micelle packing model, where micelles pack together in a cubic lattice.^{9,10} A gel is formed when the volume fraction of micelles is greater than 0.53.¹¹

Herein we report that a biofunctional zwitterionic oligopeptide (GRGD)-conjugated Pluronic copolymer showed a unique nanoassembly pattern as well as thermosensitive sol-to-gel transition. RGD not only facilitates the cell adhesion and the internalization of drugs or carriers but also contributes the enhanced permeability and retention (EPR) of a drug carrier in the tumor tissue.¹² A series of

oligopeptide-conjugated F127 derivatives were synthesized, and their self-assembly patterns were investigated as a function of temperature. The unique nanoassembly mechanism of the cell adhesive zwitterionic GRGD system is suggested, and its cytocompatibility is proved for tissue engineering application in the future.

EXPERIMENTAL SECTION

Materials. Pluronic F127 (MW 12 600), stannous octoate, *N*-hydroxysuccinimide (NHS), dicyclohexylcarbodiimide, 4-(dimethylamino)pyridine, triethylamine, anhydrous toluene, anhydrous tetrahydrofuran, dimethylformamide, and ethyl ether were used as received from Sigma-Aldrich. 4-Methacryloxyethyl trimellitic anhydride (4-META; SMC Co., Korea) was used as received. GRGD, GRGL, and GFGD were purchased from Anigen Inc., Korea. Glycolide was purchased from Polysciences, Inc. and purified using ethyl acetate prior to use. Fetal bovine serum (FBS), Dulbecco's Modified Eagle's Medium (DMEM), penicillin/streptomycin, trypsin, and phosphate buffered saline (PBS) were obtained from GIBCO, Inc.

Received: January 3, 2011

Revised: February 18, 2011

Published: March 11, 2011

Synthesis of F127 Derivatives. Pluronic F127 (F; 9.0 g, 0.70 mmol) was dissolved in anhydrous toluene (150.0 mL), and the solvent was distilled off to a final volume of 30 mL. Glycolide (G; 0.41 g, 3.5 mmol) was then added to the solution, and an additional 20 mL of toluene was distilled off to remove the residual water from the reaction mixture. Stannous octoate (1.0 mg, 2.0 μ mol) was then added to start the polymerization, and the mixture was stirred at 130 °C for 15 h. Diethyl ether was added to precipitate the product, which was filtered and dried under high vacuum. The final yield was about 90%.

The tetraglycolic acid end-capped F127 (FG; 8.0 g, 0.61 mmol) was dissolved in anhydrous toluene (150 mL), and the solvent was distilled off to a final volume of 50 mL. To the solution were added 4-META (M; 0.45 g, 1.46 mmol), 4-(dimethylamino)pyridine (0.074 g, 6.1 mmol), and triethylamine (87 μ L, 0.61 mmol). After 15 h of stirring at room temperature, the product was isolated by precipitation in diethyl ether. The polymer (FGM) was filtered and dried under vacuum. The final yield was about 80%.

Oligopeptide-grafted FGM (FGM-OligoP) copolymer was synthesized in two steps:^{13–15} (1) NHS activation of carboxyl groups of FGM and (2) addition of oligopeptides. FGM (3.0 g, 0.22 mmol) and NHS (0.78 g, 6.6 mmol) were dissolved in anhydrous THF (20 mL). To the solution were added dicyclohexylcarbodiimide (1.38 g, 6.6 mmol) and 4-(dimethylamino)pyridine (5.5 mg, 0.045 mmol). The mixture was stirred at room temperature for 15 h. Dicyclohexylurea byproduct was removed by filtration, and the remaining solution was poured into diethyl ether to precipitate the product. The polymer was redissolved in THF and then precipitated by slow addition of diethyl ether. The product was filtered and dried under vacuum. The final yield was about 70%.

The NHS-activated FGM (1.5 g, 0.11 mmol) and GRGD (110 mg, 0.275 mmol) were dissolved in *N,N*-dimethylformamide (10 mL) and stirred at room temperature for 24 h. The final product (FGM-GRGD) was precipitated by adding chilled methanol (100 mL). Other oligopeptides, GRGL and GFGL, were similarly conjugated to NHS-activated FGM. The final yield was about 60%.

Instrumentation. ¹H NMR (200 MHz NMR; Varian) was used to calculate the polymers composition. ¹³C NMR (500 MHz NMR; Varian) spectra of the polymer aqueous solution were investigated as a function of temperature in a range of 10–50 °C by a step of 10 °C. The polymer solution was equilibrated for 20 min at each step. The FTIR measurements were performed using a JASCO615 FTIR spectrometer in the frequency range 400–4000 cm^{−1} with a resolution of 4 cm^{−1}. The MALDI-TOF mass spectra of polymers were obtained by a mass spectrometer (Voyager-DE STR; Applied Biosystems, Foster, CA) equipped with a nitrogen laser emitting pulsed UV light at 337 nm and operated at an acceleration voltage of 20 kV in the reflector mode. 5 μ L of polymer matrix solution (1.0 mg/mL) consisting of α -cyano-4-hydroxycinnamic acid solution (4.0 mg/mL) of 60/40 (v/v) acetonitrile/water mixture containing 0.1% trifluoroacetic acid was deposited on the MALDI-TOF plate and air-dried at room temperature. All measurements were performed in a linear mode. Dynamic light scattering (DLS) and zeta potential of polymers in DI water were measured by a Malvern Nano ZS model using a He–Ne laser (633 nm), with data analysis by the automeasure software. The instrument was calibrated with an aqueous polystyrene dispersion of particles of 60 nm.

Micellization Study. Critical micelle concentration (CMC) and critical micelle temperature (CMT) were determined by the hydrophobic dye (1,6-diphenyl-1,3,5-hexatriene) solubilization.^{16,17} The dye solution in methanol (10.0 μ L at 0.4 mM) was injected into an aqueous solution (1.0 mL) in a polymer concentration range of 0.01–5.0 wt %. The absorption spectra of these solutions were recorded between 300 and 500 nm at room temperature as concentration for CMC increased or at 0.1 wt % as temperature for CMT measurement increased. The crossing points of the two extrapolated straight lines were defined as the CMC or the CMT of the polymers.

Sol–Gel Transition. The sol–gel transition of the polymer aqueous solution was investigated by dynamic mechanical analyzer (Thermo Haake, Rheometer RS 1) and the test tube inverting method.¹⁸ For dynamic mechanical analysis, the aqueous polymer solution (20.0 wt %) was placed between parallel plates of 25 mm diameter and a gap of 0.5 mm. The data were collected under a controlled stress of 4.0 dyn/cm² and a frequency of 1.0 rad/s at the heating rate of 0.5 °C/min. For the test tube inverting method, 0.5 mL of the FGM–GRGD aqueous solution was put in the test tube with an inner diameter of 10 mm. The transition temperature was determined by flow (sol)–nonflow (gel) criterion with a temperature increment of 1 °C per step. Each data point is an average of three measurements.

Specimen Preparation for Cryo-Transmission Electron Microscopy (Cryo-TEM). Specimens were prepared by applying 4–6 μ L of each sample solution on a grid (quantifoil purchased from Ted Pella, Inc., 300 mesh copper grid with 2 μ m perforated holes) and keeping the grid in the Vitrobot (FEI) for 30 min at a designated temperature (10–50 °C) and humidity (98–100%). The grid was then blotted with filter paper for 3–25 s and plunged immediately into the liquid ethane solution. The vitrified specimens were then studied on a FEI Tecnai G2 TEM at 200 kV with a Gatan cryoholder maintained below −170 °C. Images were recorded on an Ultrascan 2K \times 2K CCD camera and were processed using the Digital Micrograph software package.

In Vitro Chondrocyte Viability. Chondrocytes were isolated from the knee articular cartilage of 4-week-old New Zealand white rabbits by collagenase digestion.¹⁹ The isolated chondrocytes were monolayer-cultured in DMEM containing 10% FBS and 1% penicillin/streptomycin under 5% CO₂ at 37 °C atmosphere. After the cells were subcultured twice, they were harvested by trypsinization, resuspended in a fresh medium, and then seeded into 96-well culture plates at 5000 cells/well. The F127, FGM, and FGM–GRGD polymers were dissolved in the medium with a concentration of 10.0 mg/mL in a separate vial as the stock solutions. The solutions were sterilized by filtration through 0.2 μ m filters (Nalgene, Rochester, NY). The polymer solutions were diluted to the specified concentrations, in a range of 0.01–10.0 mg/mL. After 24 h, the culture medium was replaced by 200 μ L of F127, FGM, and FGM–GRGD solutions with a different concentration. After incubation for 24 h, 20 μ L of CCK-8 solution (Dojindo, Kumamoto, Japan) was added to each well, and the cells were incubated for 3 h under the conditions of 37 °C, 5% CO₂, and 95% humidity. The absorbance (*A*) of the medium was measured at 450 nm relative to 600 nm with ELISA (VERSAmax, Molecular Devices, Sunnyvale, CA). Relative cell viability (%) to control wells was calculated by $A_{\text{test}}/A_{\text{control}} \times 100$. F127 and PLL were used for comparison. Cell viability in polymer aqueous solutions was confirmed using a Live/Dead viability/cytotoxicity kit (Molecular Probes, Eugene, OR). Each sample was incubated in PBS containing 2 μ M calcein-AM and 4 μ M ethidium homodimer-1 for 30 min and was directly visualized by confocal microscopy. All images were captured using a confocal laser scanning microscope (FV1000/IX81, Olympus, Tokyo, Japan).

RESULTS AND DISCUSSION

Synthesis. Starting with the commercially available Pluronic F127, a triblock copolymer of (ethylene glycol)₉₉–(propylene glycol)₆₅–(ethylene glycol)₉₉, glycolide was polymerized on its hydroxyl end groups using stannous octoate as a catalyst (Figure 1).^{13,14} The number of glycolic acid repeating units was controlled by the molar ratio of the monomer vs F127, and the resulting oligo-glycolic acid moiety functions as a biodegradable component when applied as a biomaterial. 4-META, being used as a dental adhesive, was then coupled to hydroxyl end groups to give both carboxylic acid and methacrylate at the same time. These

Table 1. List of Polymers Studied

polymer	composition ^a	M_n	
		calcd ^b	MALDI
F127	F127	12 600	12 900
FGM	4-META-GA ₄ -F127-GA ₄ -4-META	13 670	13 670
FGM-GRGD	DGRG-4-META-GA ₄ -F127-GA ₄ -4-META-GRGD	14 440	14 360
FGM-GRGL	LGRL-4-META-GA ₄ -F127-GA ₄ -4-META-GRGL	14 440	14 540
FGM-GFGD	DGFG-4-META-GA ₄ -F127-GA ₄ -4-META-GFGD	14 420	14 360

^a GA is the glycolic acid in the repeating unit. ^b The calculated M_n is the molecular weights of polymers assuming that M_n of F127 is 12 600 Da, and the exact structures of each polymer are shown in Table 1.

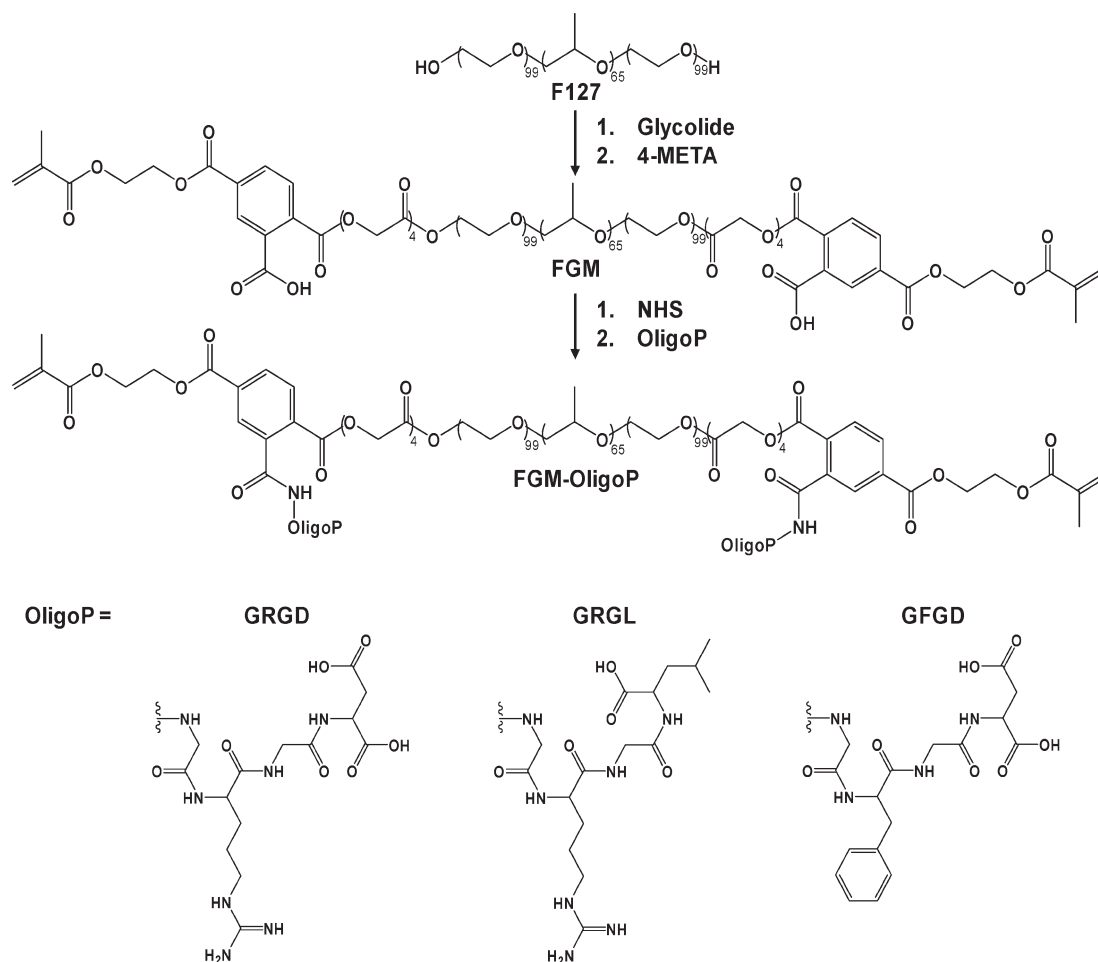


Figure 1. Synthetic diagram of oligopeptide-conjugated FGM (FGM-OligoP).

functionalities are useful for conjugating peptides and cross-linking, when necessary. To the resulting copolymer (FGM), oligopeptide of GRGD was conjugated using the NHS activation of its carboxylic acids.^{14,15} Other oligopeptides, GRGL and GFGD, were then conjugated to FGM for comparison. The final oligopeptide-conjugated copolymers were designated as FGM-GRGD, FGM-GRGL, and FGM-GFGD, respectively. FTIR spectra of FGM-GRGD showed the ester bond (C=O stretching at 1760 cm⁻¹), amide I (1660 cm⁻¹), and amide II (1570 cm⁻¹) coming from FGM and GRGD components, respectively (Figure S1). The conversion of F127 to FGM could be quantitatively analyzed by the acryl peak of 4-META at 5.5–6.2 ppm (CH₂=C(CH₃)) and

methyl peak of poly(propylene glycol) at 0.9–1.1 ppm (CH-(CH₃)CH₂O) in the ¹H NMR spectra. However, the conjugation of GRGD to FGM could not be identified by ¹H NMR spectra due to the overlap of the peaks of GRGD and FGM in the ¹H NMR spectra. MALDI-TOF spectra show the progress of the reactions from F127 to FGM-OligoP by the increase in the number-average molecular weights (M_n) from 12 900 Da to 14 360–14 540 Da (Table 1 and Figure 2). The calculated M_n in Table 1 is the molecular weights of polymers assuming that M_n of F127 is 12 600 Da, and the exact structures of each polymer are shown in Table 1.

Nanoassembly of Oligopeptide-Conjugated Copolymers. Similar to F127, FGM and FGM-GRGD easily formed micelles in

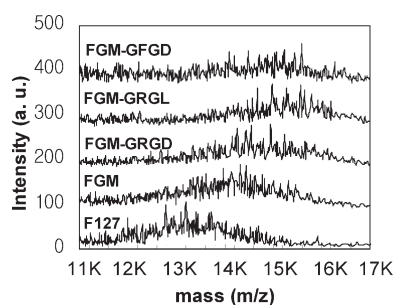


Figure 2. MALDI-TOF mass spectra of F127, FGM, and FGM-OligoP.

deionized water at room temperature. The CMC of F127, FGM, and FGM-GRGD was determined to be 1.5–2.0, 0.5–1.0, and 0.1–0.5 wt %, respectively, at 24 °C by the dye solubilization method (Figure S2).¹⁷ DLS shows the average size of the particles (d_{mp} ; most probable diameter). DLS demonstrated that FGM underwent unimer ($d_{mp} \sim 5$ nm)-to-micelle ($d_{mp} \sim 10$ nm) transition at around 35 °C (Figure 3a). The unimer-to-micelle transition temperature and the size of FGM were similar to those of F127 (35 °C, $d_{mp} \sim 7 \rightarrow \sim 16$ nm), indicating that the additional tetraglycolic acid and 4-META units did not affect the assembly behavior of FGM, while only lowering its CMC as a result of the added hydrophobicity. On the other hand, FGM-GRGD showed micellar transition ($d_{mp} \sim 7$ to ~ 60 nm) at 25 °C, followed by large aggregates ($d_{mp} \sim 150$ nm) at 25–30 °C (Figure 3a). The large aggregates disassembled to small micelles ($d_{mp} \sim 20$ nm) at 35–50 °C (Table 2). The size transition was reversible during repeated cycles of temperatures between 30 and 40 °C (Figure 3b).

To investigate the nature of the nanoassembly, zeta potential of FGM-GRGD (0.1 wt %) was measured as a function of temperature and compared with those of F127 and FGM. F127 is neutral, and its zeta potential was close to zero in a temperature range of 10–50 °C. FGM has two carboxylic acid groups that ionize in deionized water, and hence its zeta potential was negative, –23 mV at 10 °C, and ranged between –23 and –24 mV when heated to 50 °C, suggesting that the degree of ionization was not significantly changed in a temperature range of 10–50 °C. However, the zeta potential of FGM-GRGD varied as the temperature increased from 10 to 50 °C: –13 mV (10 °C), –7 mV (30 °C), and –11 mV (50 °C) (Figure 3c). These significant changes might be related to the nanoassembly of copolymers. Surface charge with both cations and anions could interact in an ion-pair forming mechanism, thus compensatively neutralize the surface charge to form large aggregates. The decrease in the apparent negative charge facilitates the nanoassembly as the temperature increases from 10 to 30 °C. As the temperature increases above 35 °C, the negative charge develops and the large aggregates disassemble into micelles.

Similar to FGM-GRGD, zwitterionic FGM-GRGL underwent unimer ($d_{mp} \sim 8$ nm)-to-large aggregate ($d_{mp} \sim 160$ nm)-to-micelle ($d_{mp} \sim 20$ nm) transitions, whereas anionic FGM-GFGD underwent unimer ($d_{mp} \sim 7$ nm)-to-micelle ($d_{mp} \sim 20$ nm) transition only as the temperature increase (Figure 3d). The differences in assembly patterns might result from the different charge interactions of the conjugated oligopeptides.

To further understand the charge effects of the oligopeptides, polymer assembly was examined as a function of pH. The pH of the solutions was adjusted by the addition of HCl or NaOH in deionized water where the polymer was dissolved. We monitored the apparent sizes of the polymers by DLS at pH = 1.5, 6.0, and

Table 2. Number of Charges in Polymers and Transitions of Polymer Aqueous Solutions (0.1 wt %)

polymers	number of charges ^a		transitions ^b (10 °C \rightleftharpoons 30 °C \rightleftharpoons 50 °C)
	cation	anion	
F127	0	0	U \rightleftharpoons M \rightleftharpoons M
FGM	0	2	U \rightleftharpoons M \rightleftharpoons M
FGM-GRGD	2	4	U \rightleftharpoons MN \rightleftharpoons M
FGM-GFGD	0	4	U \rightleftharpoons M \rightleftharpoons M
FGM-GRGL	2	2	U \rightleftharpoons MN \rightleftharpoons M

^a Counted based on guanidinium group of Arg, carboxyl group of Asp, and carboxyl group of C-terminal. ^b U = unimer, M = micelle, and MN = micellar nanoassembly.

12.5 (Figure 3e). At pH = 1.5, the FGM-GRGD with a net positive charge formed a large assembly ($d_{mp} \sim 1.1 \mu\text{m}$) at 25 °C. At pH = 6.0, where the FGM-GRGD exists in a zwitterionic form, a large assembly ($d_{mp} \sim 250$ nm) was observed over a temperature range of 25–35 °C. However, when the pH was increased to the pK_a of the guanidinium group of GRGD ($pK_a = 12.5$),²⁰ thereby reducing the number of guanidinium groups of GRGDs to a deprotonated form, no large aggregates were found and only showed unimer ($d_{mp} \sim 7$ nm)-to-micelle ($d_{mp} \sim 20$ nm) transition. The large aggregate formation at pH = 1.5 might come from hydrogen bonding between carboxylic acid groups of oligopeptides and ethylene oxide or propylene oxide groups of FGM as in poly(styrene-*co*-maleic anhydride)-*graft*-poly(ethylene glycol).²¹ At pH = 6.0, only zwitterionic oligopeptide modified FGM developed large aggregates. A similar trend in pH dependence was observed for the zwitterionic FGM-GRGL. However, FGM-GFGD with no zwitterionic character underwent unimer-to-micelle transition in a pH range of 1.5–12.5 (Figure S3). To conclude, the ionic interactions between zwitterions play an important role in the large aggregate formation. When the ionic interactions and hydrophobicity of copolymers are in a delicate balance, micelle aggregation occurs and the aggregates can grow as large as 250 nm in size.

Thermosensitive Sol-to-Gel Transitions. Sol-to-gel transitions of aqueous solutions of F127, FGM, and FGM-GRGD (20.0 wt %) were compared. The transition temperatures of F127, FGM, and FGM-GRGD were found to be 22, 38, and 17 °C, respectively (Figure 4a). The introduction of the hydrophobic moieties to F127 disturbs its effective micelle packing mechanism, resulting in interference with the gel formation. Therefore, sol-to-gel transition temperature of FGM aqueous solution was found to be higher than that of F127. A similar increase in sol–gel transition temperature was reported for oligolactide-conjugated Pluronic and oligocaprolactone-conjugated Pluronic.^{22,23} Such an increase in sol-to-gel transition temperature and a decrease in gel modulus by the hydrophobically modified Pluronics have been a concern for biomedical applications as an injectable gel. On the contrary, currently our FGM-GRGD has showed a significant decrease in sol–gel transition temperature in comparison to Pluronic F127, without loss of gel modulus. In order to elucidate the phase behavior of FGM-GRGD, cryo-transmission electron microscopy (cryo-TEM) image of the polymer aqueous solution was studied as a function of temperature and concentration. To compare morphologies of FGM-GRGD in a sol and gel state by cryo-TEM, an aqueous solution (20.0 wt %) of the polymer was incubated for 30 min at 10 and 30 °C, which are below and above the sol–gel transition temperature of 17 °C,

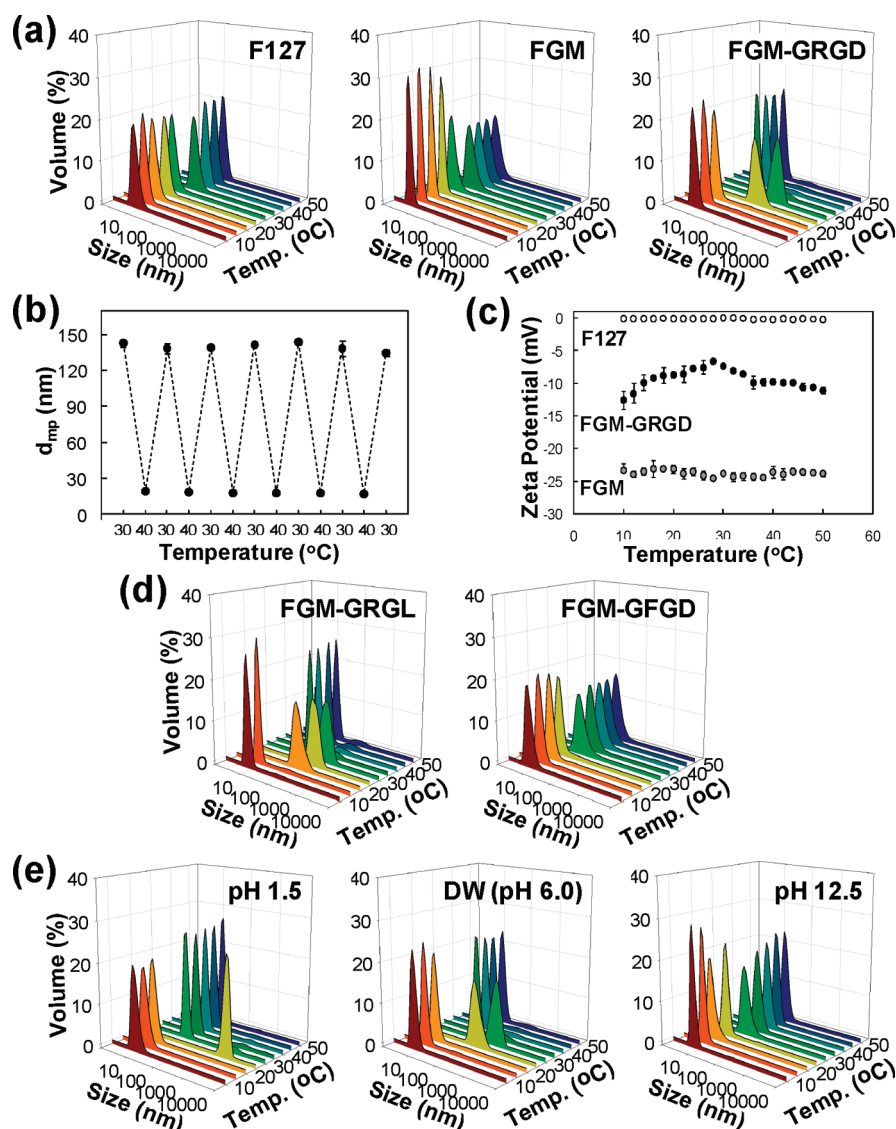


Figure 3. Changes of apparent sizes and zeta potential of polymers in water. (a) Apparent sizes of 0.1 wt % of F127, FGM, and FGM–GRGD as a function of temperature. (b) Changes in apparent size of FGM–GRGD (0.1 wt %) assembly in a heating–cooling cycle ($n = 3$). (c) Zeta potential of F127, FGM, and FGM–GRGD aqueous solutions (0.1 wt %) as a function of temperature. (d) Effect of the oligopeptide sequence on the assembly of FGM–OligoP. Apparent sizes of FGM–GRGL and FGM–GFGD in water (0.1 wt %) were shown as a function of temperature. (e) Apparent sizes of FGM–GRGD in water (0.1 wt %) as a function of temperature at pH 1.5, 6.0, and 12.5.

respectively. Cryo-TEM images of each vitrified sample revealed that the “sol state” was composed of micelles, with 20 nm in size, similar to F127 micelles in its sol state,²⁴ while the “gel state” was full of large aggregates with micrometer size which were observed as nanoassemblies of smaller micelles (50–150 nm) (Figure 4b). On the other hand, the micelle size of anionic FGM–GFGD (20.0 wt %) was observed to be 30 nm at 30 °C, and it was found that FGM–GFGD did not develop any large polymer aggregates (Figure 4c). The radial assembly behavior of FGM–GRGD is unusual among Pluronic derivatives, and this phenomenon occurred by fine-balancing of charge interactions and hydrophobic aggregation of FGM–GRGD. As the temperature increases to 50 °C, the large aggregates dissociate into small micelles with 40 nm in size (Figure 4b). As the zwitterionic FGM–GRGD concentration was increased from 0.1 → 5.0 → 20.0 wt % at 30 °C, the size of aggregate increased from 110 nm → 500 nm → 1.1 μ m (Figure 4d).

The relationship between temperature and hydrophobicity was further supported by the ¹³C NMR spectra of FGM–GRGD aqueous solution (20.0 wt % in D₂O). The peaks of ethylene glycol and propylene glycol repeating units observed at 71.5–72.5 ppm were gradually broadened and downfield shifted as the temperature increased from 10 to 50 °C. This observation suggests that the molecular motion of the Pluronic block of FGM–GRGD significantly decreases with temperature rise due to the dehydration of Pluronic block at high temperature (Figure S4).¹⁸

Mechanism of Nanoassembly. On the basis of the above observation, the assembly pattern of FGM–GRGD was schematically presented in Figure 5. At low temperature (10 °C), FGM–GRGD exists as unimers or micelles; however, they form large aggregates as the temperature increases due to the dehydration of PEG/PPG blocks and the decrease in the magnitude of the zeta potential that can reduce charge repulsion of GRGD block. As the

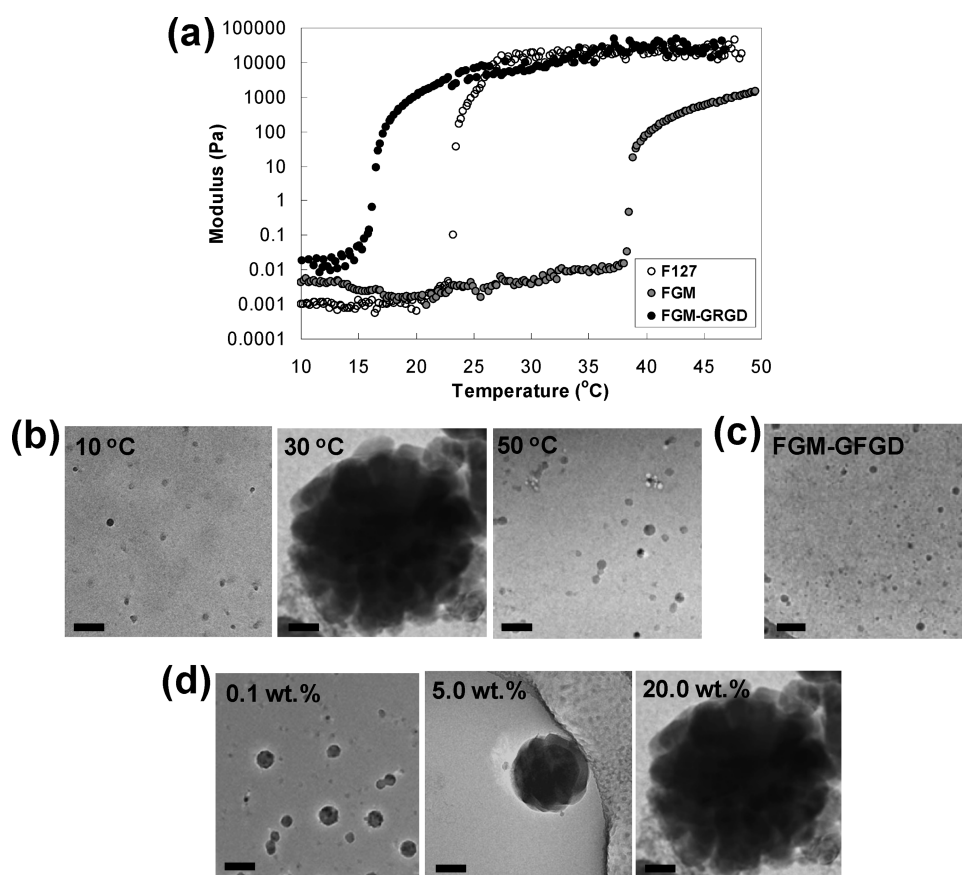


Figure 4. Sol–gel transition and radial growth in water. (a) Changes in the modulus of the F127, FGM, and FGM–GRGD aqueous solutions (20.0 wt %) as the temperature increases from 10 to 50 °C. Cryo-TEM images of the FGM–GRGD aqueous solution (20.0 wt %) at 10, 30, and 50 °C (b), FGM–GFGD aqueous solutions (20.0 wt %) at 30 °C (c), and FGM–GRGD aqueous solutions as a function of concentration at 30 °C (d). Scale bar is 200 nm.

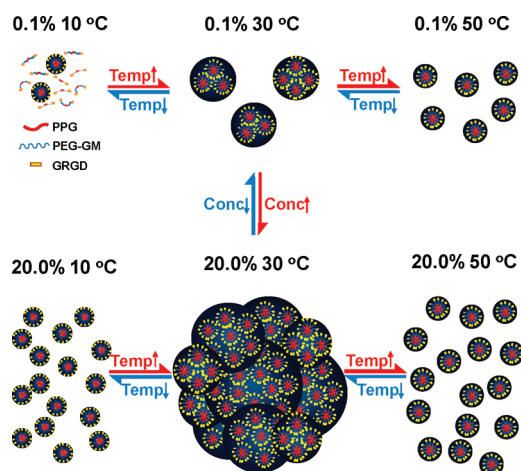


Figure 5. Proposed mechanism for self-assembly of FGM–GRGD as a function of temperature and concentration.

temperature further increases (>45 °C), the large aggregates dissociate into micelles due to densification of micelles through increased hydrophobicity,²⁵ kinetic energy,²⁶ and the increased charge repulsion as shown by negative zeta potential of FGM–GRGD. At high polymer concentration at a temperature of 30 °C, the aggregates associate to form a gel. The gel transforms to sol in

accordance with dissociation of the aggregates at both low and high temperatures of 10 and 50 °C (Figure S5). These changes in assembly are thermally reversible.

Cytocompatibility. In order to evaluate the biocompatibility of the FGM–GRGD copolymer, the viability of chondrocytes in copolymer solution was investigated. After the incubation of chondrocytes with each polymer such as poly(L-lysine) (PLL), F127, FGM, and FGM–GRGD for 24 h, the cytotoxicity was analyzed using the Cell Counting Kit-8 (CCK-8) method.²⁷ In comparison to the negative control, PLL, FGM–GRGD has shown high cell viability ($>95\%$) which is similar to that with the positive control, F127, while FGM alone showed significantly low cell viability at high concentration (10 mg/mL) (Figure S6a), suggesting that RGD moieties provides cells with biocompatibility as well as its well-known cell adhesive property.²⁸ In addition, Live/Dead staining support the viability results in each polymer solution as a function of concentration (0.01–10 mg/mL) (Figure S6b).

CONCLUSIONS

To conclude, zwitterionic FGM–GRGD copolymer reversibly formed a unique unimer, large aggregates, and micelles by varying temperature from 10 to 50 °C. The thermosensitive transition of FGM–GRGD is caused by the cooperative action of ionic interactions and hydrophobic interactions. In addition, our current zwitterionic modified polymer aqueous solution decreases the sol-to-gel transition temperature while keeping the

gel modulus. These points are distinguished from previous hydrophobic modified Pluronic that show an increase in the sol-to-gel transition temperature and a decrease in the gel modulus, thus limiting the biomedical applications as a gel depot system. This copolymer with cytocompatibility is a promising candidate as a biocompatible material. By fine control of intermolecular forces in such zwitterionic oligopeptide conjugated Pluronic, one can design an interesting assembly as well as thermosensitive sol-to-gel transition for drug delivery and tissue regeneration.

■ ASSOCIATED CONTENT

S Supporting Information. ^1H NMR spectra of F127, FGM, and FGM-GRGD in DMSO- d_6 ; FTIR spectra of F127, FGM, and FGM-GRGD; UV-vis spectra of 1,6-diphenyl-1,3,5-hexatriene in the F127, FGM, and FGM-GRGD aqueous solutions (0.1 wt %) for critical micelle concentration of F127, FGM, and FGM-GRGD; apparent sizes of FGM-GRGL and FGM-GFGD in water (0.1 wt %) as a function of temperature at pH 1.5, 6.0, and 12.5; ^{13}C NMR spectra of FGM-GRGD in D_2O as a function of temperature; phase diagram of FGM-GRGD aqueous solutions; chondrocyte viability in F127, FGM, and FGM-GRGD aqueous solutions as a function of concentration determined by CCK-8; confocal microscopic images of monolayer cultured chondrocytes analyzed using a Live/Dead kit. This material is available free of charge via the Internet at <http://pubs.acs.org>.

■ AUTHOR INFORMATION

Corresponding Author

*E-mail: dkh@kist.re.kr (D.K.H.); bjeong@ewha.ac.kr (B.J.).

■ ACKNOWLEDGMENT

This research was supported by Pioneer Research Center Program through the National Research Foundation of Korea funded by the Ministry of Education, Science and Technology (2010-0002170), a grant from the Fundamental R&D Program for Core Technology of Materials funded by the Ministry of Knowledge Economy, Republic of Korea (K00060-282), and National Research Foundation of Korea (Grants 2010-0000832 and R31-2008-000-10010-0). B.G.C. was supported by the Seoul Science Fellowship. We thank the Advanced Analysis Center at the Korea Institute of Science and Technology (KIST) for access to cryo-TEM. We also thank Prof. Jeffrey A. Hubbell at Swiss Federal Institute of Technology (EPFL), Switzerland, for valuable discussions.

■ REFERENCES

- (1) Feng, X.; Fryxell, G. E.; Wang, L. Q.; Kim, A. Y.; Liu, J.; Kemner, K. M. *Science* **1997**, *276*, 923–926.
- (2) Malenfant, P. R. L.; Wan, J. L.; Taylor, S. T.; Manoharan, M. *Nature Nanotechnol.* **2007**, *2*, 43–46.
- (3) Piao, Y.; Kim, J.; Na, H. B.; Kim, D.; Baek, J. S.; Ko, M. K.; Lee, J. H.; Shokouhimehr, M.; Hyeon, T. *Nature Mater.* **2008**, *7*, 242–247.
- (4) Kim, J. K.; Lee, E.; Lim, Y. B.; Lee, M. *Angew. Chem.* **2008**, *120*, 4740; *Angew. Chem., Int. Ed.* **2008**, *47*, 4662–4666.
- (5) Jeong, B.; Bae, Y. H.; Lee, D. S.; Kim, S. W. *Nature* **1997**, *388*, 860–862.
- (6) Ding, Z. L.; Fong, R. B.; Long, C. J.; Stayton, P. S.; Hoffman, A. S. *Nature* **2001**, *411*, 59–62.
- (7) Nishida, K.; Yamato, M.; Hayashida, Y.; Watanabe, K.; Yamamoto, K.; Adachi, E.; Nagai, S.; Kikuchi, A.; Maeda, N.; Watanabe, H.; Okano, T.; Tano, Y. *New Engl. J. Med.* **2004**, *351*, 1187–1196.
- (8) Escobar-Chavez, J. J.; Lopez-Cervantes, M.; Naik, A.; Kalia, Y. N.; Quintanar-Guerrero, D.; Ganem-Quintanar, A. *J. Pharm. Pharm. Sci.* **2006**, *9*, 339–358.
- (9) Rill, R. L.; Locke, B. R.; Liu, Y. J.; Van Winkle, D. H. *Proc. Natl. Acad. Sci. U.S.A.* **1998**, *95*, 1534–1539.
- (10) Willet, N.; Gohy, J.-F.; Lei, L.; Heinrich, M.; Auvray, L.; Varshney, S.; Jerome, R.; Leyh, B. *Angew. Chem.* **2007**, *119*, 8134; *Angew. Chem., Int. Ed.* **2007**, *46*, 7988–7992.
- (11) Mortensen, K.; Pedersen, S. *Macromolecules* **1993**, *26*, 805–812.
- (12) Temming, K.; Schiffelers, R. M.; Molema, G.; Kok, R. J. *Drug Resist. Update* **2005**, *8*, 381–402.
- (13) Deng, C.; Tian, H.; Zhang, P.; Sun, J.; Chen, X.; Jing, X. *Biomacromolecules* **2006**, *7*, 590–596.
- (14) Park, S. Y.; Lee, Y.; Bae, K. H.; Ahn, C. H.; Park, T. G. *Macromol. Rapid Commun.* **2007**, *28*, 1172–1176.
- (15) Hersel, U.; Dahmen, C.; Kessler, H. *Biomaterials* **2003**, *24*, 4385–4415.
- (16) Booth, C.; Attwood, D. *Macromol. Rapid Commun.* **2000**, *21*, 501–527.
- (17) Alexandridis, P.; Holzwarth, J. F.; Hatton, T. A. *Macromolecules* **1994**, *27*, 2414–2425.
- (18) Hwang, M. J.; Suh, J. M.; Bae, Y. H.; Kim, S. W.; Jeong, B. *Biomacromolecules* **2005**, *6*, 885–890.
- (19) Unger, F.; Wittmar, M.; Kissel, T. *Biomaterials* **2007**, *28*, 1610–1619.
- (20) Stryer, L. *Biochemistry*, 4th ed.; W.H. Freeman & Co.: New York, 1995; p 43.
- (21) Yin, X.; Stover, H. D. H. *Macromolecules* **2002**, *35*, 10178–10181.
- (22) Xiong, X. Y.; Tam, K. C.; Gan, L. H. *Polymer* **2005**, *46*, 1841–1850.
- (23) Joo, M. K.; Park, M. H.; Choi, B. G.; Jeong, B. *J. Mater. Chem.* **2009**, *19*, 5891–5905.
- (24) Lam, Y. M.; Grigorieff, N.; Goldbeck-Wood, G. *Phys. Chem. Chem. Phys.* **1999**, *1*, 3331–3334.
- (25) Li, H.; Yu, G. E.; Price, C.; Booth, C. *Macromolecules* **1997**, *30*, 1347–1354.
- (26) Arotcarena, M.; Heise, B.; Ishaya, S.; Laschewsky, A. J. *Am. Chem. Soc.* **2002**, *124*, 3787–3793.
- (27) Ishiyama, M.; Miyazono, Y.; Sasamoto, K.; Ohkura, Y.; Ueno, K. *Talanta* **1997**, *44*, 1299–1305.
- (28) Gallant, N. D.; Lavery, K. A.; Amis, E. J.; Becker, M. L. *Adv. Mater.* **2007**, *19*, 965–969.